



## OPEN Halofuginone prevents inflammation and proliferation of high-altitude pulmonary hypertension by inhibiting the TGF- $\beta$ 1/Smad signaling pathway

Jiangtao Wang<sup>1,2,6</sup>, Lina Guan<sup>1,6</sup>, Jian Yu<sup>3,6</sup>, Bohua Ma<sup>4</sup>, Huihua Shen<sup>1</sup>, Guozhu Xing<sup>1</sup>, Yawei Xu<sup>1</sup>, Qiufang Li<sup>1</sup>, Juan Liu<sup>1</sup>, Qin Xu<sup>5</sup>, Wenhui Shi<sup>5</sup>, Jia He<sup>1</sup>, Yixuan Huang<sup>1</sup>, Dongfeng Yin<sup>1</sup>✉, Wu Li<sup>1,2</sup>✉ & Rui Wang<sup>1</sup>✉

The inflammatory response of lung tissue and abnormal proliferation of pulmonary artery smooth muscle cells are involved in the pathogenesis of high-altitude pulmonary hypertension (HAPH). Halofuginone (HF), an active ingredient derivative of Chang Shan (*Dichroa febrifuga* Lour. [Hydrangeaceae]), has antiproliferative, antihypertrophic, antifibrotic, and other effects, but its protective effects on HAPH remains unclear. In the present study, we evaluated the efficacy of HF on HAPH by establishing a 6000 m HAPH rat model. Male Sprague–Dawley rats were divided into normoxia, normoxia + halofuginone (1 mg/kg), hypoxia, and hypoxia + halofuginone (1 mg/kg) groups. The results showed that HF (1 mg/kg) could prevent hypoxia-induced hemodynamic abnormalities, right ventricular hypertrophy, and pulmonary vascular remodeling in rats. We further detected the expression levels of inflammatory factors interleukin (IL)-1 $\beta$ , IL-6, tumor necrosis factor- $\alpha$  (TNF- $\alpha$ ) and proliferative/antiproliferative indicators proliferating cell nuclear antigen (PCNA), cyclin-dependent kinase 6 (CDK6), Cyclin D1, p21 in lung tissue, and found that HF could attenuate the lung tissue inflammatory response and proliferative response in HAPH rats. In addition, we also examined the expression levels of transforming growth factor- $\beta$ 1 (TGF- $\beta$ 1), Smad2/3 and p-Smad2/3 in lung tissue, and found that HF exerted therapeutic effects by inhibiting the TGF- $\beta$ 1/Smad signaling pathway.

**Keywords** Hypoxia, Pulmonary hypertension, Remodeling, Inflammation, Proliferation, TGF- $\beta$ 1/Smad signaling pathway

According to statistics, more than 140 million people worldwide live at high altitude above 2500 m for a long time, and up to 10% of them suffer from chronic mountain sickness, among which high-altitude pulmonary hypertension (HAPH) is a malignant pulmonary vascular disease. HAPH is mainly characterized by hypoxic pulmonary vasoconstriction and hypoxic pulmonary vascular remodeling, which causes persistent increase of pulmonary circulatory resistance and eventually leads to right heart failure or even death. HAPH belongs to the third category in the classification of pulmonary arterial hypertension (PAH)<sup>1–3</sup>. Despite years of research into the pathogenesis and drugs of HAPH, the prognosis of patients remains poor<sup>4</sup>. At present, the most effective way for HAPH remains removal from the hypoxic environment, but this is clearly unrealistic for generations of residents<sup>2</sup>. Pharmacological treatment for HAPH includes: calcium receptor antagonists, sGC stimulators, prostacyclin and its analogues, PDE5 inhibitors, endothelin-1 receptor antagonists, etc. Although these drugs can improve hemodynamics and quality of life for patients, most of them have a single target and are expensive, limiting the treatment of HAPH patients to a certain extent<sup>4</sup>. Therefore, searching for safe, effective, inexpensive and multi-target therapeutic drugs is the direction of our future research.

<sup>1</sup>General Hospital of Xinjiang Military Command, 359 North Friendship Road, Sayibak, Ürümqi 830000, Xinjiang, China. <sup>2</sup>School of Medicine, Shihezi University, Shihezi 832000, China. <sup>3</sup>Tumor Hospital of Xinjiang Medical University, Ürümqi 830000, China. <sup>4</sup>Department of Pharmacy, Qingyang People's Hospital, Qingyang 745000, China. <sup>5</sup>Xinjiang Key Laboratory of Special Environmental Medicine, Ürümqi 830000, China. <sup>6</sup>Jiangtao Wang, Lina Guan and Jian Yu contributed equally to this work. ✉email: ydf1112@163.com; goodli002@163.com; urumqi@126.com

Halofuginone (HF) is a synthetic halogenated derivative of febrifugine, a natural quinazolinone alkaloid which can be found in the Chinese herb Chang Shan (*Dichroa febrifuga* Lour. [Hydrangeaceae]), which exhibits pharmacological effects such as antiproliferative, antihypertrophic, and antifibrotic; its earliest application was in the treatment of chicken coccidiosis<sup>5</sup>. In recent years, studies have found that HF has shown therapeutic effects in lung cancer<sup>6</sup>, melanoma bone metastases<sup>7</sup>, fibrotic diseases<sup>8</sup>, osteoarthritis<sup>9</sup>, leukemia<sup>10</sup>, and other diseases. Notably, the efficacy by HF is associated with the modulation of the transforming growth factor- $\beta$  (TGF- $\beta$ )/Smad signaling pathway. In addition, Jain et al. found through in vivo and in vitro studies that HF activated potassium channels and inhibited different types of calcium channels in pulmonary artery smooth muscle cells (PASCs) to mediate pulmonary vasodilation, and that HF also mediated antiproliferative effect via inhibiting the PI3K/Akt/mTOR signaling pathway<sup>11</sup>.

Abnormal proliferation and apoptotic resistance of PASCs are the main mechanisms responsible for pulmonary vascular remodeling, which play an important role in the progression of HAPH<sup>12</sup>. The TGF- $\beta$ 1/Smad signaling pathway is involved in the proliferation and differentiation of PASCs, and hypoxia up-regulates TGF- $\beta$ 1 expression in lung tissue, which in turn activates the phosphorylation of downstream Smad2/3 protein, leading to abnormal proliferation of PASCs and accelerating the pathological process<sup>13,14</sup>. In addition, the TGF- $\beta$ 1/Smad signaling pathway can also participate in the progression of PAH by regulating other signaling pathways<sup>15</sup>.

The role and mechanism of HF in HAPH have not been reported yet. We attempted to investigate the protective effects and potential mechanisms of HF by establishing a rat model of HAPH, in order to provide a reference basis for the clinical treatment of patients with HAPH.

## Results

### Effects of HF on hemodynamics in HAPH rats

The success of rat modeling was assessed by measuring RVSP and mPAP in each group of rats after 4 weeks. The results showed that exposure to hypoxic environment at high altitude for 4 weeks caused an increase in RVSP compared with the Nor group ( $54.56 \pm 1.95$  mmHg vs.  $28.95 \pm 1.53$  mmHg;  $P < 0.001$ ), and a concomitant increase in mPAP ( $35.28 \pm 1.18$  mmHg vs.  $19.66 \pm 0.94$  mmHg;  $P < 0.001$ ), suggesting that the HAPH rat model was successfully established. The RVSP and mPAP of HAPH rats were lower than those of the Hyp group when HF was gavaged once a day during 4 weeks ( $35.24 \pm 0.80$  mmHg vs.  $54.56 \pm 1.95$  mmHg,  $23.49 \pm 0.49$  mmHg vs.  $35.28 \pm 1.18$  mmHg;  $P < 0.001$ ). The treatment showed a hemodynamic effect, reducing the RVSP and mPAP (Fig. 1A–C, Tab S1). In addition, to evaluate the effects of HF on hemodynamics in rats under normoxic environment, we set up the Nor+HF group. The results showed that the RVSP and mPAP of rats in the Nor+HF group were not different from those in the Nor group ( $26.86 \pm 1.95$  mmHg vs.  $28.95 \pm 1.53$  mmHg,  $18.39 \pm 1.19$  mmHg vs.  $19.66 \pm 0.94$  mmHg;  $P > 0.05$ ), which suggested that HF had no significant effects on hemodynamics of rats in the normoxic condition (Fig. 1A–C, Tab S1).

### Effects of HF on right ventricular hypertrophy in HAPH rats

After hemodynamic measurement, the degree of right ventricular hypertrophy in rats was assessed by calculating the RVHI (%). The results showed that the RVHI of rats exposed to hypoxia for 4 weeks was increased compared with the Nor group ( $54.87 \pm 4.50$  vs.  $23.33 \pm 1.83$ ;  $P < 0.001$ ). The RVHI of HAPH rats was lower than those of the Hyp group after administration of HF by gavage for 4 weeks ( $38.68 \pm 5.13$  vs.  $54.87 \pm 4.50$ ;  $P < 0.001$ ). The above results suggested that HF could attenuate right ventricular hypertrophy in HAPH rats (Fig. 1D, Tab S1). In addition, the Nor+HF group was set up to assess whether HF had effects on right ventricle of rats in the normoxic environment. The results showed no significant difference in RVHI between the Nor+HF group and Nor group ( $21.25 \pm 1.43$  vs.  $23.33 \pm 1.83$ ;  $P > 0.05$ ), and these results suggested that HF had no significant effects on right ventricle of rats under normoxic condition (Fig. 1D, Tab S1).

### Effects of HF on pulmonary vascular remodeling in HAPH rats

To evaluate the effects of HF on pulmonary vascular remodeling in HAPH rats, lung tissues were collected from rats in each group and observed with HE staining. HE staining results showed that the hypoxic environment led to thickening of the walls and narrowing of the lumen of small pulmonary artery in rats, while intervention with HF improved these pathological changes (Fig. 2A). Meanwhile, the wall thickness and wall area of small pulmonary artery in pathological sections were further measured, and WT% and WA% were calculated, respectively. The results showed that compared with the Nor group, exposure to hypoxia for 4 weeks resulted in an increase in WT% and WA% of small pulmonary artery ( $42.83 \pm 9.13$  vs.  $19.74 \pm 2.27$ ,  $65.28 \pm 7.53$  vs.  $43.81 \pm 4.85$ ;  $P < 0.001$ ), whereas these values were decreased after administration of HF ( $24.76 \pm 3.89$  vs.  $42.83 \pm 9.13$ ,  $51.71 \pm 7.28$  vs.  $65.28 \pm 7.53$ ;  $P < 0.001$ ). The above results suggested that HF could improve pulmonary vascular remodeling in HAPH rats (Fig. 2B,C, Tab S2). In addition, by setting the Nor+HF group, we also found that HF had no significant effects on pathological morphology, WT% and WA% of small pulmonary artery in rats under normoxic atmosphere ( $16.08 \pm 4.15$  vs.  $19.74 \pm 2.27$ ,  $41.79 \pm 4.11$  vs.  $43.81 \pm 4.85$ ;  $P > 0.05$ ; Fig. 2B,C, Tab S2), so we affirmed that HF did not change the physiological/normal morphology.

### Effects of HF on inflammatory factors in lung tissue of HAPH rats

The inflammatory response is relevant to the development of HAPH, so we measured the levels of inflammatory factors IL-1 $\beta$ , IL-6 and TNF- $\alpha$  in lung tissue of rats in each group using ELISA kits. The results showed that the levels of inflammatory factors IL-1 $\beta$ , IL-6 and TNF- $\alpha$  in lung tissue of rats exposed to hypoxia for 4 weeks were up-regulated compared with the Nor group ( $618.61 \pm 71.21$  ng/L vs.  $444.54 \pm 58.41$  ng/L,  $525.76 \pm 100.91$  ng/L vs.  $386.74 \pm 63.93$  ng/L,  $509.38 \pm 62.31$  ng/L vs.  $327.60 \pm 35.98$  ng/L;  $P < 0.01$  or  $P < 0.001$ ). After oral administration of HF for 4 weeks, the levels of inflammatory factors IL-1 $\beta$ , IL-6 and TNF- $\alpha$  in lung tissue were down-

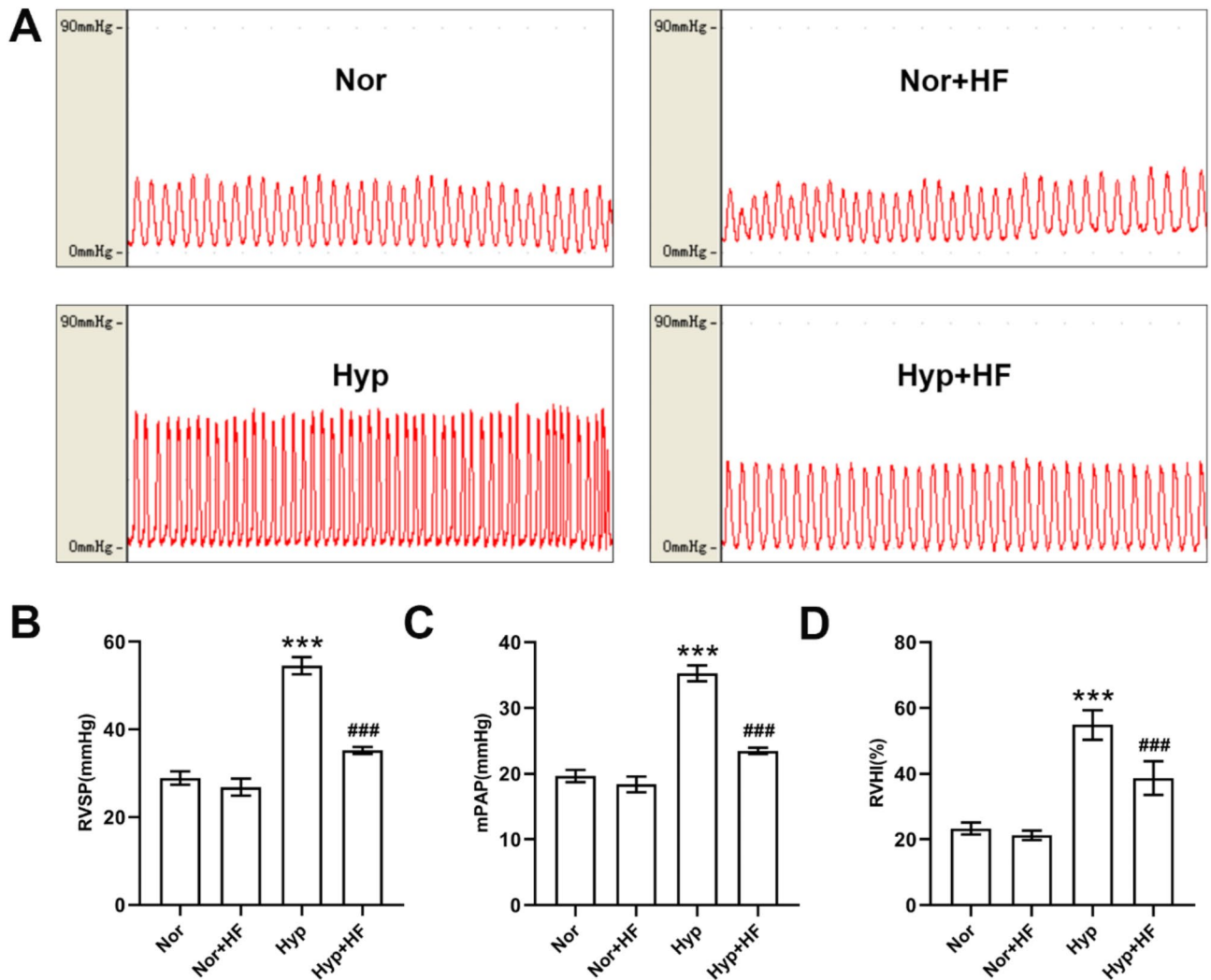


**Fig. 1.** Effects of HF on hemodynamics and right ventricular hypertrophy in HAPH rats. (A) RVSP waveforms of rats in each group. (B–D) Changes in RVSP, mPAP, RVHI of rats in each group. The data are expressed as the mean  $\pm$  SD,  $n = 10$  per group. \*\*\* $P < 0.001$  vs. the Nor group; ### $P < 0.001$  vs. the Hyp group. RVSP: right ventricular systolic pressure; mPAP: mean pulmonary artery pressure; RVHI: right ventricular hypertrophy index.

regulated compared with the Hyp group ( $520.00 \pm 66.85$  ng/L vs.  $618.61 \pm 71.21$  ng/L,  $437.50 \pm 74.96$  ng/L vs.  $525.76 \pm 100.91$  ng/L,  $433.33 \pm 50.07$  ng/L vs.  $509.38 \pm 62.31$  ng/L;  $P < 0.05$ ). These results suggested that HF could inhibit inflammatory response in lung tissue of HAPH rats (Fig. 3A–C, Tab S3). In addition, to assess the effects of HF on inflammatory factors in lung tissue of rats at plain, the Nor + HF group was set. The results showed that the levels of inflammatory factors IL-1 $\beta$ , IL-6 and TNF- $\alpha$  in lung tissue of rats were not statistical significance between the Nor + HF group and Nor group ( $434.44 \pm 34.72$  ng/L vs.  $444.54 \pm 58.41$  ng/L,  $338.18 \pm 12.28$  ng/L vs.  $386.74 \pm 63.93$  ng/L,  $308.13 \pm 17.90$  ng/L vs.  $327.60 \pm 35.98$  ng/L;  $P > 0.05$ ), which suggested that HF had no significant effects on inflammatory factors in lung tissue of rats under normoxic condition (Fig. 3A–C, Tab S3).

#### Effects of HF on pulmonary vascular proliferation in HAPH rats

$\alpha$ -SMA is an expressed protein of PSMCs and is often used as a marker protein to identify PSMCs. To evaluate the effects of HF on pulmonary vascular proliferation in HAPH rats, the expression of  $\alpha$ -SMA in small pulmonary artery of rats was detected by IHC staining, and the expressions of PCNA, CDK6, Cyclin D1, p21 in lung tissue of rats were also detected by WB. IHC staining results showed that the expression of  $\alpha$ -SMA in pulmonary artery of rats exposed to hypoxic condition for 4 weeks was higher ( $P < 0.05$ ), whereas intervention with HF reversed this alteration ( $P < 0.05$ ; Fig. 4A, Tab S4). Meanwhile, WB results showed that the expressions of proliferative proteins PCNA, CDK6, Cyclin D1 were higher ( $P < 0.05$  or  $P < 0.01$ ) and the expression of antiproliferative protein p21 was lower ( $P < 0.01$ ) in lung tissue of rats exposed to hypoxia compared with the Nor group. Compared with the Hyp group, the expressions of PCNA, CDK6, Cyclin D1 in lung tissue of rats were decreased ( $P < 0.05$ ) and the expression of p21 was increased ( $P < 0.05$ ) after administration of HF by gavage for 4 weeks. The above results suggested that HF could suppress the abnormal proliferation of PSMCs induced

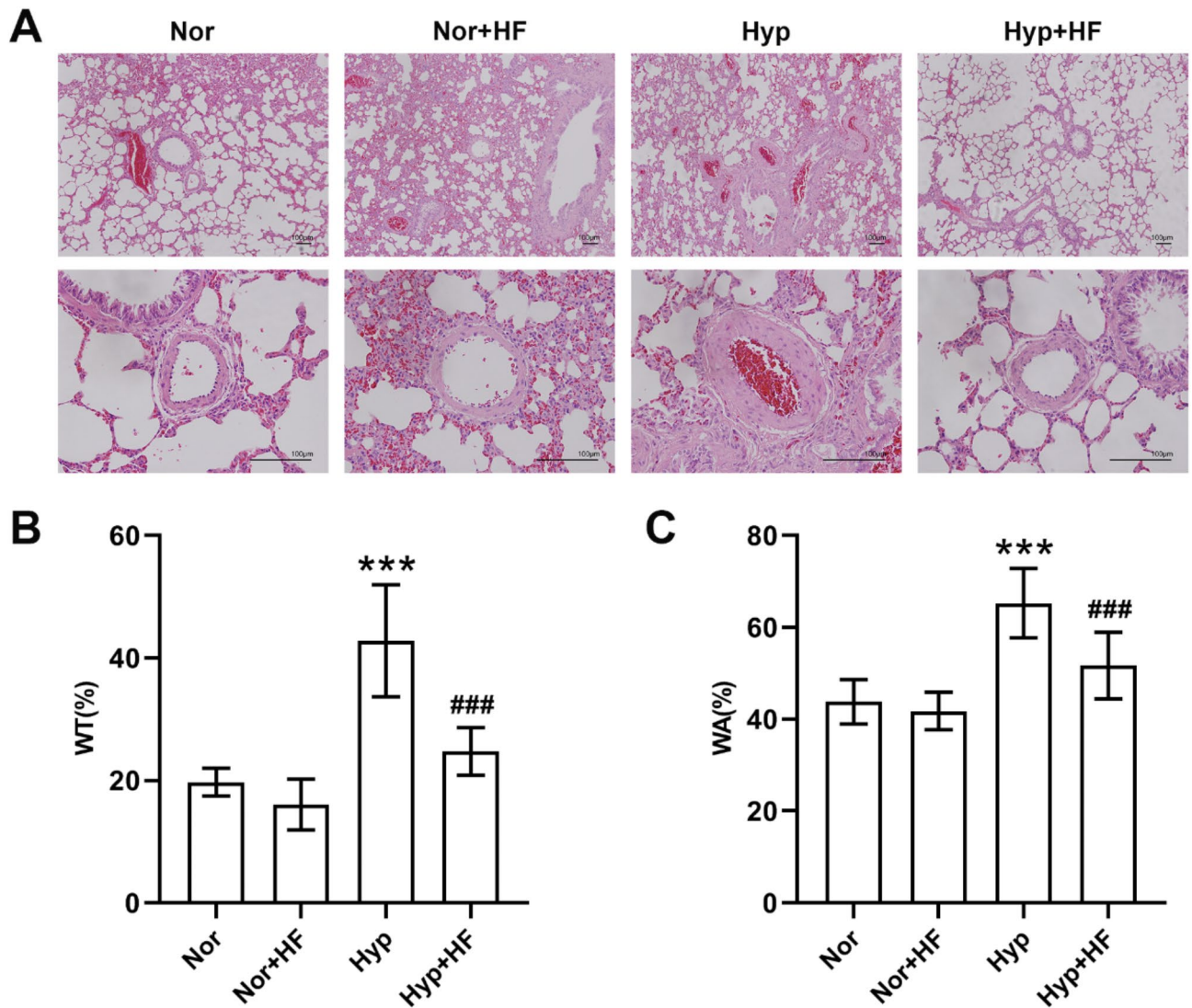


**Fig. 2.** Effects of HF on pulmonary vascular remodeling in HAPH rats. (A) Representative pulmonary arterioles of left lung tissues were stained by HE in each group of rats (magnification  $\times 100/400$  and scale bar = 100  $\mu\text{m}$ ). (B,C) Changes in WT%, WA% of small pulmonary arteries in each group of rats. The data are expressed as the mean  $\pm$  SD,  $n = 7$  per group. <sup>\*\*\*</sup> $P < 0.001$  vs. the Nor group; <sup>###</sup> $P < 0.001$  vs. the Hyp group. WT: wall thickness; WA: wall area.

by the hypoxic environment at plateau (Fig. 4B–E, Tab S5). In addition, by setting up the Nor + HF group, we also found that HF had no significant effects on the expressions of PCNA and CDK6 ( $P > 0.05$ ), but the expressions of Cyclin D1 (decreased) and p21 (increased) were statistically different ( $P < 0.05$  or  $P < 0.01$ ; Fig. 4B–E, Tab S5).

#### Effects of HF on the TGF- $\beta$ 1/Smad signaling pathway related proteins of lung tissue in HAPH rats

The TGF- $\beta$ 1/Smad signaling pathway participates in the progression of HAPH, and it remains unclear about whether the protective effects of HF on HAPH are related to this pathway. Therefore, we examined the expressions of TGF- $\beta$ 1/Smad signaling pathway related proteins in lung tissue of rats using WB. The results showed that the expressions of TGF- $\beta$ 1 and p-Smad2/3 were increased in lung tissue of rats exposed to hypoxic atmosphere compared with the Nor group ( $P < 0.05$  or  $P < 0.01$ ), while the expression of Smad2/3 had no statistical change ( $P > 0.05$ ). Compared with the Hyp group, the expression of TGF- $\beta$ 1 and the phosphorylation level of Smad2/3 in lung tissue of rats were down-regulated after administration of HF by gavage ( $P < 0.05$ ). These results suggested that the treatment of HAPH by HF was associated with reducing the activation of TGF- $\beta$ 1/Smad signaling pathway (Fig. 5A,B, Tab S6). In addition, we also found that HF had no significant effects on the expressions of TGF- $\beta$ 1, Smad2/3 and p-Smad2/3 in lung tissue of rats under normoxic condition by setting up the Nor + HF group ( $P > 0.05$ ; Fig. 5A,B, Tab S6).

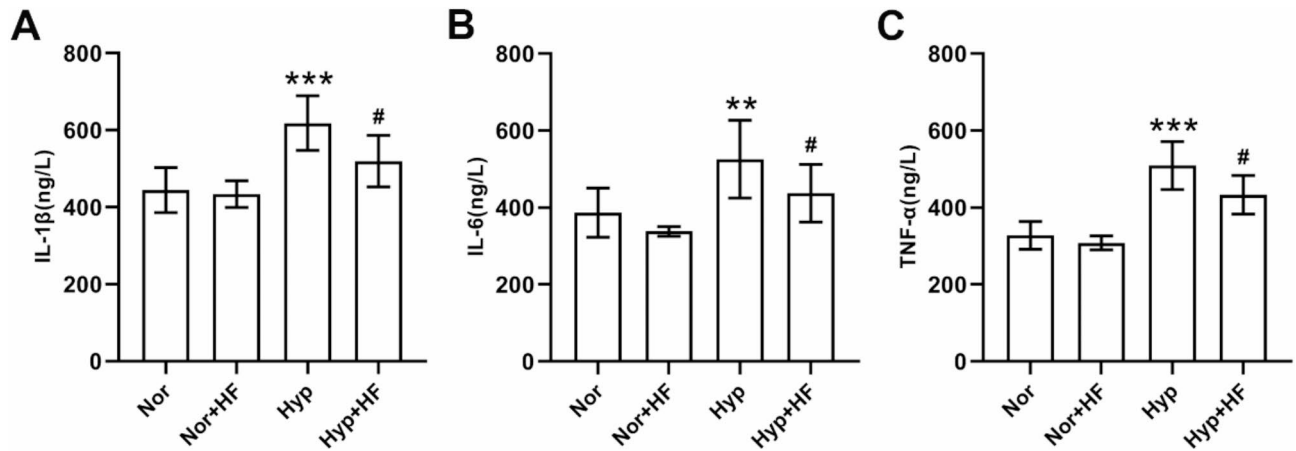


**Fig. 3.** Effects of HF on inflammatory factors in lung tissue of HAPH rats. (A–C) Changes of inflammatory factors IL-1 $\beta$ , IL-6, TNF- $\alpha$  in lung tissue of rats were detected by ELISA in each group. The data are expressed as the mean  $\pm$  SD,  $n = 5$ –6 per group. \*\* $P < 0.01$ , \*\*\* $P < 0.001$  vs. the Nor group; # $P < 0.05$  vs. the Hyp group.

## Discussion

The results of this study demonstrated that HF showed benefits during a HAPH model development through multi-targeted effects, such as reducing inflammatory factors and PSMCs proliferation in lungs of rats induced by the hypoxic environment of high altitude, and down-regulating the expression levels of TGF- $\beta$ 1/Smad signaling pathway related proteins.

HAPH is a malignant pulmonary vascular disease that develops due to incomplete adaptation of body to the hypoxic environment of high altitude. Our study successfully replicated the 6000 m HAPH rat model and found that the hypoxia-induced elevated RVSP and mPAP, right ventricular hypertrophy and pulmonary vascular remodeling in rats, which was consistent with previous findings<sup>16,17</sup>. After the intervention with HF, we found that it could reduce RVSP and mPAP, attenuate right ventricular hypertrophy, and improve pulmonary vascular remodeling in HAPH rats. In addition, we also found that HF had no obvious effects on rats in the normoxic environment. These results suggested that HF could alleviate the macroscopic indicators in HAPH rats, but what is the mechanism of its action, so we carried out further experiments and discussions.

Inflammation is involved in the occurrence and development of HAPH. It has been demonstrated that blood monocytes migrate to lung perivascular spaces and differentiate into interstitial macrophages under hypoxic environment, and these cells can further promote the inflammatory progression of PAH via secreting inflammatory factors IL-1 $\beta$ , IL-6 and TNF- $\alpha$ <sup>18</sup>. Previous studies have found that HF could inhibit inflammatory factors IL-1 $\beta$ , IL-6 and TNF- $\alpha$  in a variety of diseases. For example, HF suppressed the production of pro-inflammatory cytokines IL-1 $\beta$ , IL-6 and TNF- $\alpha$ , and thus exerting a protective effect against lipopolysaccharide (LPS)-induced endothelial dysfunction<sup>19</sup>; increased production of inflammatory cytokines IL-1 $\beta$ , IL-6 and TNF- $\alpha$  in the serum of concanavalin A (ConA)-induced liver fibrosis rat model, and oral administration of HF for 8 weeks could attenuate the inflammatory response<sup>20</sup>, the levels of pro-inflammatory cytokines IL-1 $\beta$ , IL-6 and TNF- $\alpha$  in the serum of acute viral myocarditis in suckling mice were down-regulated by HF, and the levels of anti-inflammatory cytokines were increased to exert protective effects<sup>21</sup>; by establishing the model of delayed-type hypersensitivity (DTH) in vivo and in vitro, it was found that HF was an effective immunomodulator and anti-inflammatory agent<sup>22</sup>. However, the effects of HF on HAPH-related inflammatory factors IL-1 $\beta$ , IL-6 and TNF- $\alpha$  have not been reported. In this study, the levels of IL-1 $\beta$ , IL-6 and TNF- $\alpha$  in lung tissue were significantly increased by establishing the HAPH rat model, suggesting that there was a certain correlation between inflammation and symptoms of HAPH rats. After administration of HF for 4 weeks, the symptoms of HAPH rats were effectively alleviated, and the levels of IL-1 $\beta$ , IL-6 and TNF- $\alpha$  in lung tissue were also significantly decreased, which further suggested that the effects of HF on hemodynamics, right ventricular hypertrophy and pulmonary vascular remodeling in HAPH rats might be related to the inhibition of IL-1 $\beta$ , IL-6 and TNF- $\alpha$  levels. In addition, we also found that HF had no significant effects on these indices of rats exposed to normoxic condition.

The persistent contraction and abnormal proliferation of PSMCs are the core factors in the formation of HAPH. Under normal circumstances, the proliferation and apoptosis of various cells in vivo are in a dynamic homeostasis, which is disrupted in PSMCs stimulated by hypoxic condition<sup>23</sup>.  $\alpha$ -SMA is a marker protein of PSMCs, which can reflect the degree of proliferation<sup>24</sup>. In addition, cell proliferation is achieved by regulating the cell cycle, in which proliferating cell nuclear antigen (PCNA), cyclin-dependent kinases (CDKs), cyclins and CDK inhibitors (CKIs) play a key role in regulating the process<sup>25–27</sup>. It has been shown that HF can inhibit cell proliferation by regulating cell cycle-related components. For example, in the tight-skin mouse model, cell proliferation was detected by using PCNA antibody and collagen type I probe, and local application of HF was found to inhibit the proliferation of dermal fibroblasts and reduce collagen synthesis, therefore ameliorating dermal fibrosis in mouse<sup>28</sup>; HF inhibited the cell proliferation of MCF-7 (human breast cancer cell line) via suppressing exosomal miR-31 targeting HDAC2 and regulating cellular G1/S phase components such as CDK2,

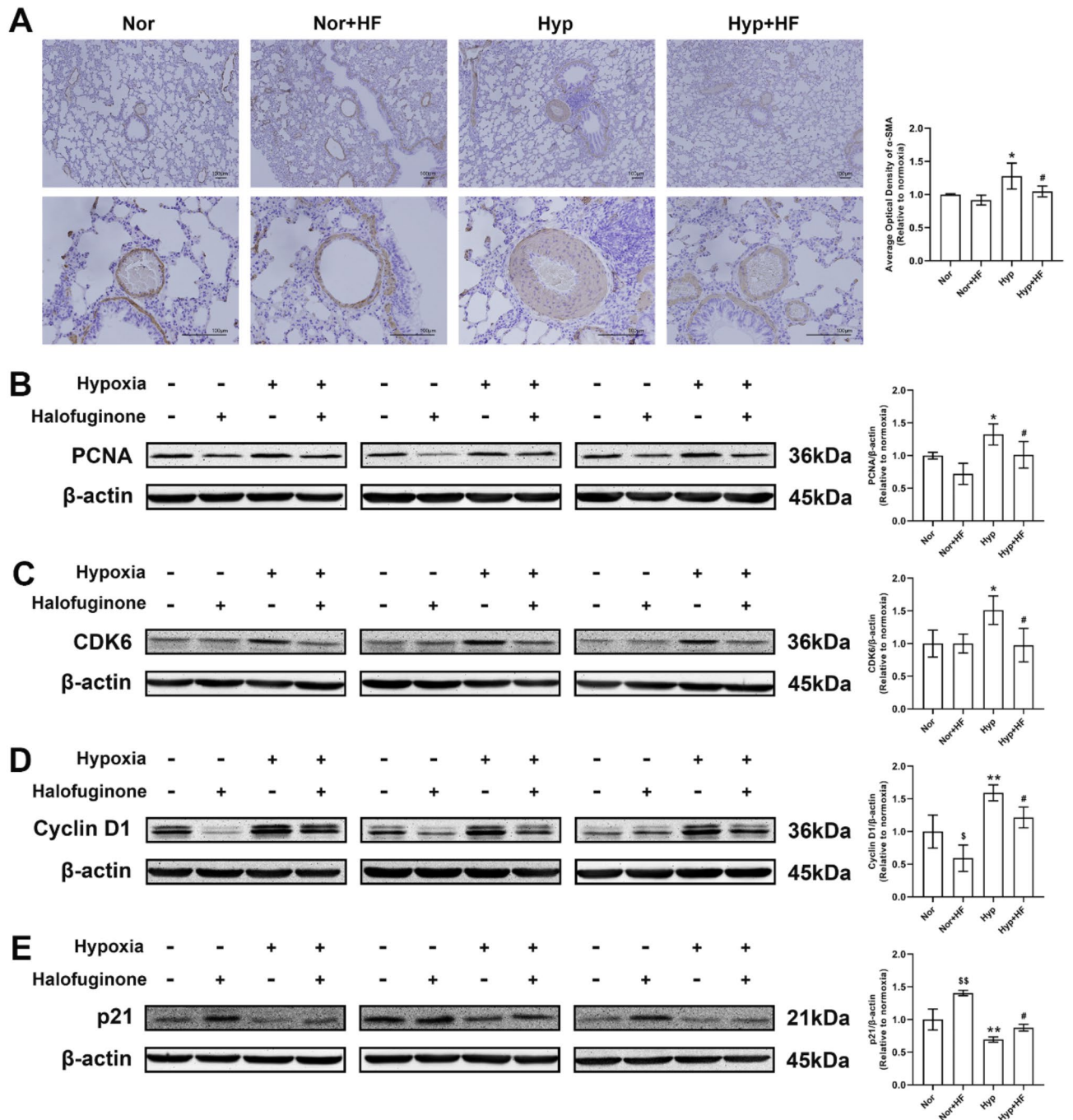


**Fig. 4.** Effects of HF on pulmonary vascular proliferation in HAPH rats. (A)  $\alpha$ -SMA expressions of representative pulmonary arterioles were stained by IHC in each group of rats (magnification  $\times 100/400$  and scale bar = 100  $\mu$ m). (B–D) Changes of proliferative indicators PCNA, CDK6, Cyclin D1 expressions in lung tissue of rats were detected by WB in each group. (E) Change of antiproliferative indicator p21 expression in lung tissue of rats was detected by WB in each group. Original blots are presented in Supplementary information. The data are expressed as the mean  $\pm$  SD, n = 3 per group.  $^{\$}P < 0.05$ ,  $^{\$\$}P < 0.01$ ,  $^*P < 0.05$ ,  $^{**}P < 0.01$  vs. the Nor group;  $^{\#}P < 0.05$  vs. the Hyp group.

Cyclin D1 and p21<sup>29</sup>; NRF2 regulated c-Myc, Cyclin D1 and Bcl-2 to promote the proliferation of cutaneous squamous cell carcinoma, and HF could enhance the antitumor effect of ALA-PDT by suppressing the expression of NRF2-associated signals<sup>30</sup>; HF arrested HepG2 and Huh7 cells (hepatocellular carcinoma cell line) from G1 to S phase by reducing the synthesis of Cyclin D1/B1 in hepatocellular carcinoma cells<sup>31</sup>. However, the role of HF in regulating cell cycle-related components has not been reported in HAPH. In the present study, we found that the hypoxic environment mediated pulmonary vascular remodeling in rats, and the important mechanism was the abnormal proliferation of PSMCs. Nevertheless, the use of HF could reduce the expression of  $\alpha$ -SMA in

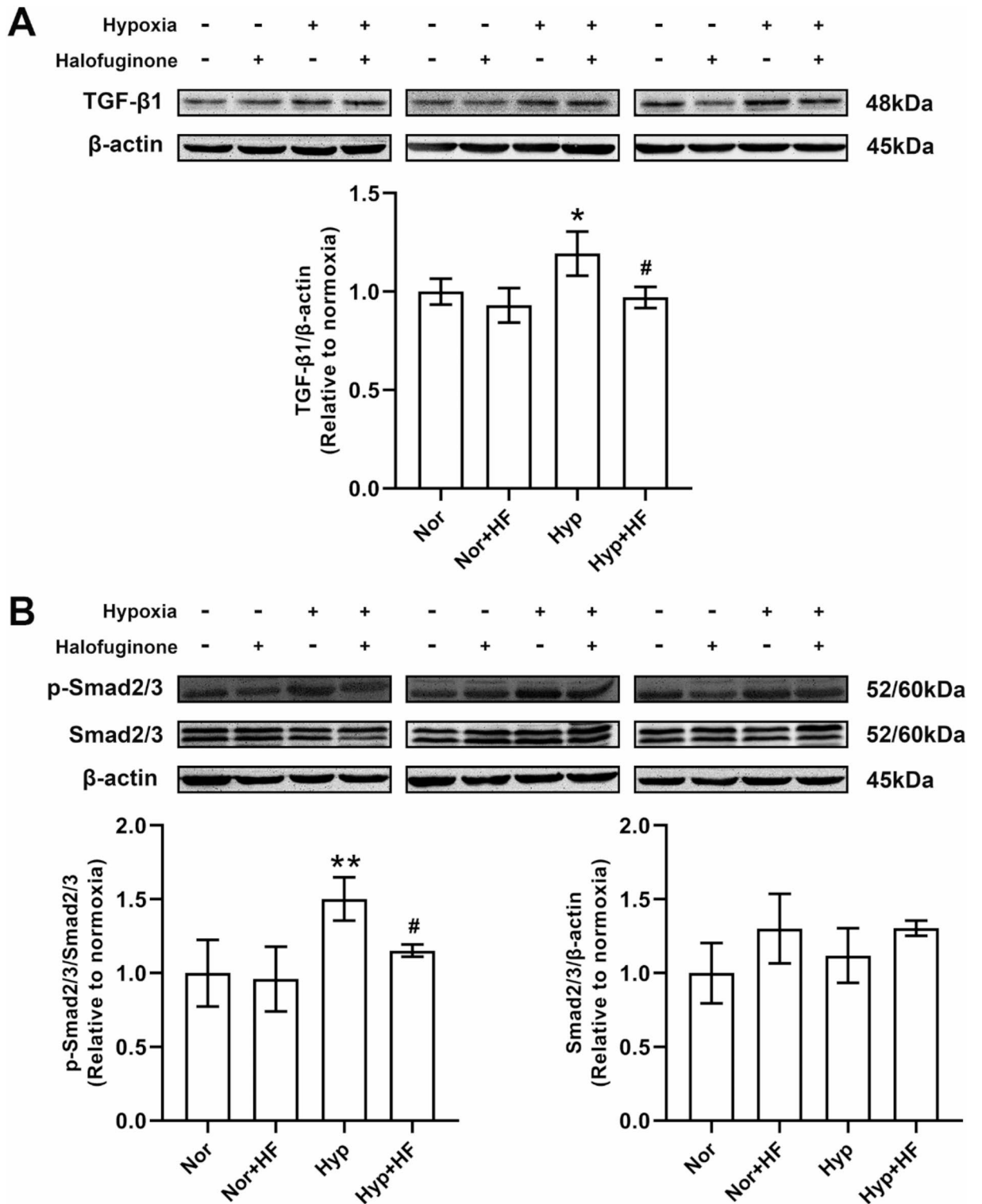


**Fig. 5.** Effects of HF on TGF-β1/Smad signaling pathway related proteins of lung tissue in HAPH rats. (A) Change of TGF-β1 expression in lung tissue of rats was detected by WB in each group. (B) Changes of p-Smad2/3 and Smad2/3 expressions in lung tissue of rats were detected by WB in each group. Original blots are presented in Supplementary information. The data are expressed as the mean ± SD, n = 3 per group. \**P* < 0.05, \*\**P* < 0.01 vs. the Nor group; #*P* < 0.05 vs. the Hyp group.

pulmonary artery, decrease the expressions of proliferative proteins PCNA, CDK6, Cyclin D1 and up-regulate the expression of antiproliferative protein p21, thus blocking the cell cycle and inhibiting the excessive proliferation of PSMCs. In addition, we also found that HF had effects on Cyclin D1 and p21 expressions in rats exposed to normoxia, but this did not cause the changes of macroscopic indicators in HAPH rats, which might be the results of multiple mechanisms acting together.

The TGF- $\beta$ 1/Smad signaling pathway is involved in the progression of HAPH<sup>32</sup>. It was found that HF could exert therapeutic effects in a variety of diseases by modulating the TGF- $\beta$ /Smad signaling pathway. For instance, in the rodent anterior cruciate ligament transection (ACLT) models, it was found that HF alleviated the progression of osteoarthritis via inhibiting the activation of TGF- $\beta$ /Smad signaling pathway and abnormal angiogenesis in subchondral bone<sup>9</sup>; HF prevented the development of melanoma bone metastases by down-regulating the TGF- $\beta$ -dependent phosphorylation levels of Smad2/3 in human melanoma cells<sup>7</sup>; in vivo and in vitro experiments revealed that HF reduced VEGF content in the bone marrow of acute promyelocytic leukemia (APL) mouse, decreased VEGF secretion and Smad2 phosphorylation in NB4 cells (APL cell line), and blocked the TGF- $\beta$  signaling pathway, thereby reducing the growth and angiogenesis of leukemia<sup>10</sup>; HF restrained the TGF- $\beta$  induced fibrotic response in fibroblasts<sup>8</sup>; in addition, HF also strengthened the antitumor effect of irradiation in lung cancer via inhibiting the TGF- $\beta$ /Smad signaling pathway<sup>6</sup>. However, no studies have reported the role of HF in HAPH-related TGF- $\beta$ 1/Smad signaling pathway. The results of this study showed that the expression levels of TGF- $\beta$ 1/Smad signaling pathway related proteins were significantly up-regulated in lung tissue of HAPH rats, suggesting that this pathway was associated with HAPH to a certain extent. After 4 weeks of intragastric administration of HF, it was found that HF could down-regulate the expression of TGF- $\beta$ 1 and the phosphorylation level of Smad2/3, and attenuate the excessive activation level of TGF- $\beta$ 1/Smad signaling pathway in HAPH, thus improving the related symptoms of HAPH rats.

The TGF- $\beta$  signaling pathway is closely associated with inflammatory and proliferative responses in PAH<sup>33</sup>. The TGF- $\beta$  superfamily consists of 33 members, of which the main ones are TGF- $\beta$ s (TGF- $\beta$ 1/2/3) and BMPs. Smad proteins are the classical downstream molecules of TGF- $\beta$  superfamily, with TGF- $\beta$ s mediating Smad2/3 phosphorylation and BMPs mediating Smad1/5/8 phosphorylation, both of which exert regulatory effects by transmitting upstream signals from the plasma membrane to the nucleus<sup>34,35</sup>. Imbalanced signaling triggered by the TGF- $\beta$  superfamily contributes to the dysregulation of vascular cell proliferation in PAH, with overactive pro-proliferative Smad2/3 signaling occurring alongside deficient antiproliferative Smad1/5/8 signaling, and its mediated inflammatory response is also involved<sup>36</sup>. Numerous studies have shown that TGF- $\beta$ 1 is most closely associated with the progression of PAH and that pulmonary vascular remodeling and PSMCs proliferation are often relieved by inhibiting the TGF- $\beta$ 1/Smad signaling pathway in PAH models<sup>14</sup>. Besides the classical Smad signaling pathway, TGF- $\beta$ 1 also plays a role in PAH by mediating non-Smad signaling pathways. For instance, TGF- $\beta$ 1 inhibited PSMCs apoptosis and further promoted the thickening of pulmonary vascular wall via activating the PI3K-Akt pathway<sup>37</sup>; calpain-2 promoted PSMCs proliferation and pulmonary vascular remodeling by up-regulating Akt phosphorylation through the intracellular TGF- $\beta$ 1/mTORC2 mechanism, which was independent of PI3K<sup>38</sup>; overexpression of TGF- $\beta$ 1 activated the RhoA/ROCK signaling pathway, thereby promoting the development of PAH<sup>39</sup>; CTRP9 exerted antiproliferative effect through the TGF- $\beta$ 1/ERK1/2 signaling pathway in hypoxia-induced PAH<sup>40</sup>. The findings indicated that the level of inflammatory factors and proliferative indexes were elevated in HAPH rats compared with normoxic rats, and at the same time, the TGF- $\beta$ 1/Smad signaling pathway was over-activated. In contrast, after intervention with HF, the expression of TGF- $\beta$ 1/Smad signaling pathway was attenuated while inflammatory and proliferative responses were also weakened in HAPH rats. Therefore, we hypothesized that HF might improve the inflammatory and proliferative responses of HAPH rats by inhibiting the TGF- $\beta$ 1/Smad signaling pathway, so as to achieve the therapeutic effects.

## Conclusion

Our results showed that HF could reduce hemodynamic parameters, attenuate right ventricular hypertrophy, and improve pulmonary vascular remodeling in HAPH rats, which be related to the inhibition of TGF- $\beta$ 1/Smad signaling pathway mediated inflammation and proliferation (Fig. 6). These findings suggest that HF is a potential drug for the treatment of HAPH, providing an experimental basis for the application of HF in HAPH, and this also offers a novel approach for the clinical treatment of HAPH patients.

## Materials and methods

### Materials

HF (purity > 97%, RH337723, R110877, CAS No. 55837-20-2; Fig. 7A) was purchased from Yien Chemical Technology Co., Ltd. (Shanghai, China) and dissolved in distilled water. Ethyl carbamate (purity > 99%) was purchased from Titan Technology Co., Ltd. (Shanghai, China) and dissolved in normal saline. Heparin sodium was purchased from First Biochemical Pharmaceutical Co., Ltd. (Shanghai, China). Rat IL-1 $\beta$  (YX-091203R), IL-6 (YX-091206R), TNF- $\alpha$  (YX-201407R) ELISA KIT were purchased from Youxuan Biotechnology Co., Ltd. (Shanghai, China). All immunohistochemical (IHC) reagents, RIPA buffer, PMSE, BCA protein assay kit, primary antibodies against  $\alpha$ -SMA (Cat. No. 19245), PCNA (Cat. No. 13110), CDK6 (Cat. No. 3136), Cyclin D1 (Cat. No. 55506), Smad2/3 (Cat. No. 8685), p-Smad2/3 (Cat. No. 8828),  $\beta$ -actin (Cat. No. 4970), and Anti-rabbit (Cat. No. 7074)/mouse (Cat. No. 7076) IgG, HRP-linked antibodies were purchased from Cell Signaling Technology (Danvers, MA, USA). Primary antibodies against p21 (Cat. No. ab109199), TGF- $\beta$ 1 (Cat. No. ab179695) were purchased from Abcam (Cambridge, MA, USA).

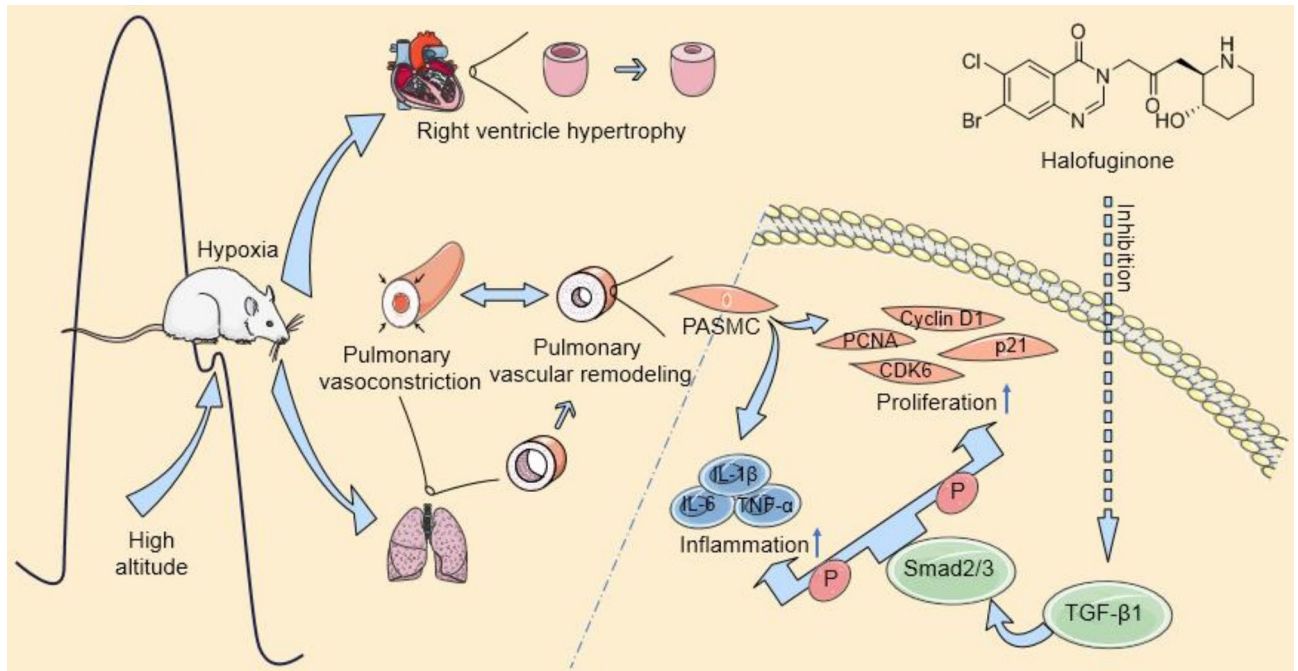


**Fig. 6.** Mechanistic diagram of HF against HAPH. Inflammation and proliferation in rats are induced by the hypoxic environment of high altitude, while HF prevents inflammation and proliferation by inhibiting the TGF- $\beta$ 1/Smad signaling pathway to exert therapeutic effects against HAPH.

### Experimental animals and ethical approval

Eight-week-old male Sprague–Dawley rats (200  $\pm$  20 g) were purchased from the Animal Experiment Center of Xinjiang Medical University [License number: SCXK (XIN) 2023-0001] and housed in the SPF-grade animal room of the General Hospital of Xinjiang Military Command for 1 week of acclimation (temperature of 22–24  $^{\circ}$ C, humidity of 40–50%, and 12 h light/dark cycle), and had free access to food and water. All animal experimental protocols were approved by the Animal Ethics Committee of the General Hospital of Xinjiang Military Command (DWLL20220303), and all experiments were performed in accordance with relevant guidelines and regulations. Also, all methods complied with the ARRIVE guidelines.

### HAPH rat model

The HAPH rat model was established by using the Northwest Special Environment Artificial Experimental Chamber (Feng Lei Oxygen Chamber Co., Ltd., Guizhou, China). Based on our previous modeling experience and the modeling methods of other units using the same type of experimental chamber<sup>16</sup>, we set the parameters as follows: simulated altitude of 6000 m, descending pressure rate of 5.0 m/s, fresh air volume demand of 50 m<sup>3</sup>/h, so that the chamber pressure reaches 47.3 kPa, temperature of 22–24  $^{\circ}$ C, humidity of 40–50%, and 12 h night/day cycle. The artificial experimental chamber was lowered to the plain height for 1 h each morning for drug administration, bedding change, feed and water supplementation for 4 weeks.

### Experimental design

The experimental animals were divided into equal size of groups using randomized and blinded method (n = 10 per group). The intragastric dose of HF was based on our previous study<sup>41</sup>: by setting up HF groups with low (0.5 mg/kg), medium (1 mg/kg) and high (2 mg/kg) doses, we finally selected the medium dose as the one to be used in this experiment. In this study (Fig. 7B), rats were randomly divided into 4 groups: (1) normoxia group (Nor): rats were placed in plain environment for 4 weeks and given equal amounts of distilled water once daily by gavage; (2) normoxia + halofuginone group (Nor + HF): rats were placed in plain environment for 4 weeks and given 1 mg/kg of HF once daily by gavage; (3) hypoxia group (Hyp): rats were placed in 6000 m artificial experimental chamber for 4 weeks and given equal amounts of distilled water once daily by gavage; (4) hypoxia + halofuginone group (Hyp + HF): rats were placed in 6000 m artificial experimental chamber for 4 weeks and given 1 mg/kg of HF once daily by gavage. The rats under normoxic environment were given the same conditions except for hypoxic environment. We set up the Nor + HF group to test whether HF would affect the levels of hemodynamics, right ventricle, pulmonary vascular wall, inflammatory factors, proliferative/antiproliferative proteins and TGF- $\beta$ 1/Smad signaling pathway related proteins in normoxic rats.

### Hemodynamic measurement

After 4 weeks, the rats were weighed and anesthetized with 20% ethyl carbamate (5 mL/kg) by intraperitoneal injection, and fixed in supine position on the operating table. The small animal ventilator (Chengdu Instrument Factory, China) was connected after endotracheal intubation, and the parameters were set as follows: respiratory

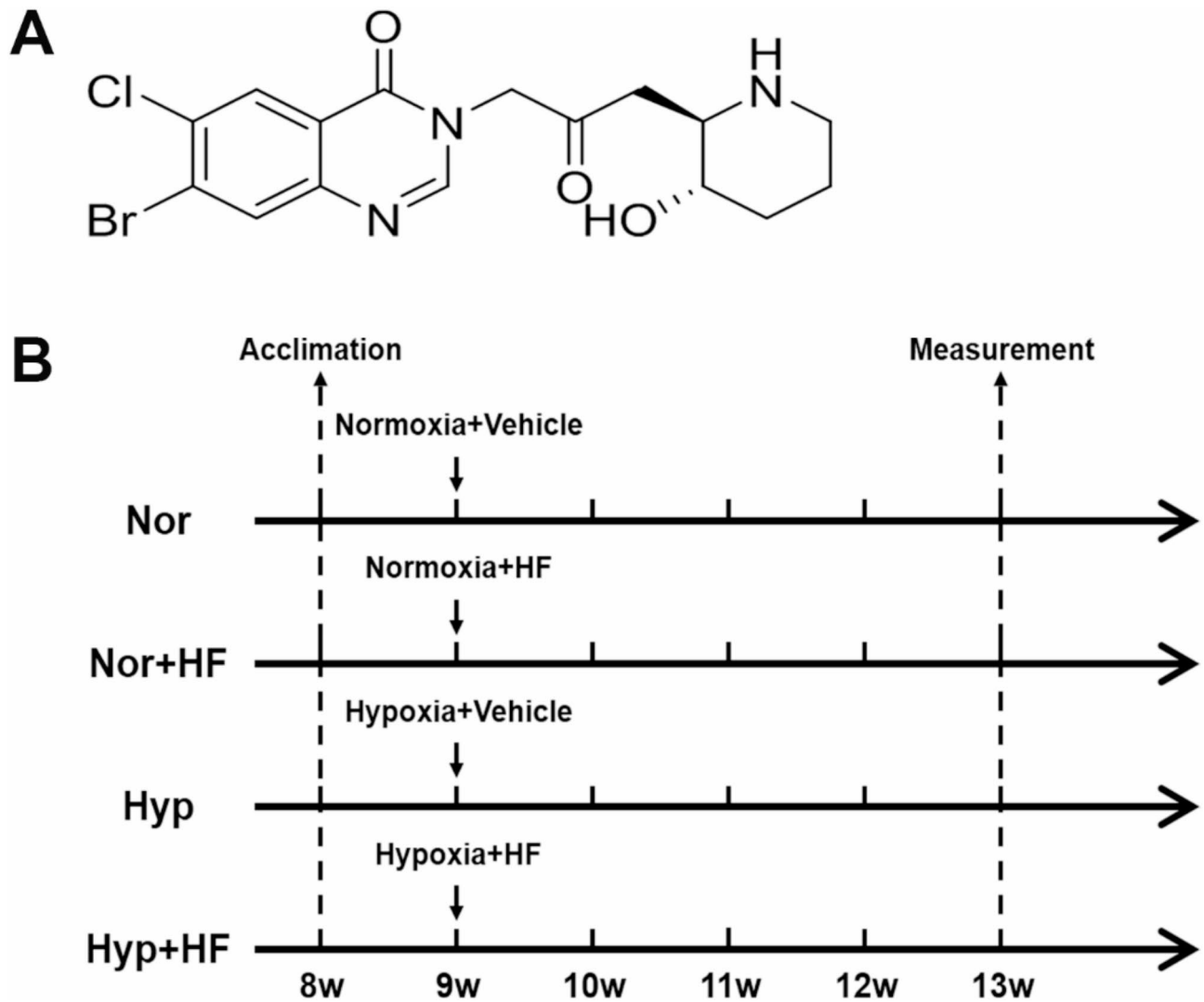


**Fig. 7.** HF and experimental protocols. (A) The chemical structure of HF. Formula:  $C_{16}H_{17}BrClN_3O_3$ ; CAS No. 55837-20-2; Mr: 414.68. (B) Experimental groups, duration of drug administration and time point of detection. Nor: normoxia group; Nor + HF: normoxia + halofuginone group; Hyp: hypoxia group; Hyp + HF: hypoxia + halofuginone group.

rate of 60 breaths/min, tidal volume of 6 mL, and respiratory ratio of 3:2. After the vital signs of rats were stabilized, the thoracic cavity was opened to fully expose the lungs and heart, and a rigid polyethylene catheter filled with heparinized saline (0.9% NaCl solution + 25 U/mL heparin) was rapidly inserted directly into the right ventricle via the diaphragm<sup>4</sup>. The other end of the catheter was connected to a pressure transducer and a physiological signal recorder (Chengdu Instrument Factory, China) to monitor the pressure changes, and the right ventricular systolic pressure (RVSP) was recorded in each group of rats after the waveform was stable. The mean pulmonary artery pressure (mPAP) was calculated by the formula:  $mPAP = 0.61 \times RVSP + 2$ <sup>11</sup>.

#### Right ventricular hypertrophy testing

After hemodynamic measurement, the rats were sacrificed with an excess of 20% ethyl carbamate and the hearts were removed. The left and right atria and the root tissues of great vessels were cut along the atrioventricular sulcus, and then the right ventricle (RV) and left ventricle + septum (LV + S) were separated along the edge of the ventricular septum. After draining with filter paper and weighing, the RVHI was calculated to reflect the degree of right ventricular hypertrophy [ $RVHI = RV/(LV + S)$ ]<sup>11</sup>.

#### Pulmonary vascular remodeling assessment

The left lung tissue of rats was isolated and fixed in 4% paraformaldehyde, trimmed along the pulmonary hilum and then embedded in paraffin. The paraffin blocks were cut into 4  $\mu$ m thick sections and stained with hematoxylin-eosin (HE). We selected 7 slices of different rats in each group and measured the parameters with ImageJ software. The small pulmonary artery (50–200  $\mu$ m) wall thickness (WT%) and wall area (WA%) were calculated to assess the degree of pulmonary vascular remodeling<sup>23,42</sup>.

### Inflammatory factors assay

After homogenizing the 0.1 g of right anterior lung lobe of rats in each group with appropriate amount of normal saline, the homogenate was centrifuged at  $4000\times g$  for 10 min at 4 °C (Thermo Scientific Hereaus FRESCO 21, Thermo Fisher Scientific, USA), and the supernatant was reserved for later use. The levels of inflammatory factors IL-1 $\beta$ , IL-6 and TNF- $\alpha$  in lung tissue of rats in each group were determined by enzyme-linked immunosorbent assay (ELISA), and the operation was carried out strictly according to the kit instructions.

### IHC staining of the small pulmonary artery

The 4  $\mu$ m paraffin-embedded left lung sections were dewaxed, rehydrated, and immersed in citrate unmasking solution for antigen repair by microwave heating to boiling. Then, the paraffin sections were blocked with the animal-free blocking solution (a blocking solution in IHC staining) for 1 h at room temperature and then incubated with primary antibody against  $\alpha$ -SMA (1:320) at 4 °C overnight, and the next day incubated with secondary antibody conjugated with anti-rabbit horseradish peroxidase for 30 min at room temperature. Finally, the sections were stained with diaminobenzidine (DAB) and counterstained with hematoxylin, and the sections were dehydrated and sealed. IHC staining of  $\alpha$ -SMA in the pulmonary artery of rats in each group was observed under the microscope (BX51, OLYMPUS, Japan), and we selected 3 slices of different rats in each group and analyzed  $\alpha$ -SMA expression using ImageJ software (IHC Profiler plug-in).

### Western blot (WB)

The right posterior lung lobe (0.1 g) of rats in each group was taken and lysed with RIPA buffer containing 1% PMSF (1 mM), and phosphatase inhibitors were added to detect phosphorylated forms of proteins. After lysate was centrifuged at  $14,000\times g$  for 10 min at 4 °C, the supernatant was collected and the protein concentration was determined by BCA protein assay kit. The protein concentration was homogenized, boiled at 100 °C for 5 min and then packed and frozen. Equal amounts of proteins were separated by SDS-PAGE gels and electrotransferred to PVDF membranes. The membranes were blocked with 5% nonfat milk at room temperature for 1 h and washed with  $1\times$  TBST three times, then incubated with primary antibodies against PCNA (1:1000), CDK6 (1:2000), Cyclin D1 (1:1000), p21 (1:1000), TGF- $\beta$ 1 (1:1000), Smad2/3 (1:1000), p-Smad2/3 (1:1000), and  $\beta$ -actin (1:1000) overnight at 4 °C. The following day, the membranes were washed with  $1\times$  TBST three times and incubated with HRP-linked secondary antibodies (1:2000) at room temperature for 1 h. After washing, the protein bands were exposed using the ChemiDoc-It 510 Imager (UVP, USA). Each experiment was repeated three times. The protein levels of bands were normalized to the levels of  $\beta$ -actin or non-phosphorylated protein.

### Statistical analysis

SPSS 25.0, GraphPad Prism 8 and ImageJ software were used for statistical analysis and plotting. The experimental data basically complied with the normal distribution. All data were expressed as mean  $\pm$  SD, one-way ANOVA was used for comparison between multiple groups. For multiple comparisons among groups, LSD-*t* test was used for homogeneous of variances and Dunnett's T3 test was used for heterogeneous of variances.  $P < 0.05$  was considered statistically significant.

### Data availability

Data is provided within the supplementary information files.

Received: 3 April 2024; Accepted: 28 January 2025

Published online: 29 January 2025

### References

- Soria, R., Egger, M., Scherrer, U., Bender, N. & Rimoldi, S. F. Pulmonary arterial pressure at rest and during exercise in chronic mountain sickness: A meta-analysis. *Eur. Resp. J.* **53**, 1802040 (2019).
- Xu, X. Q. & Jing, Z. C. High-altitude pulmonary hypertension. *Eur. Respir. Rev.* **18**, 13–17 (2009).
- Simonneau, G. et al. Haemodynamic definitions and updated clinical classification of pulmonary hypertension. *Eur. Resp. J.* **53**, 1801913 (2019).
- Chen, Y. et al. Tetramethylpyrazine: A promising drug for the treatment of pulmonary hypertension. *Br. J. Pharmacol.* **177**, 2743–2764 (2020).
- Edgar, S. A. & Flanagan, C. Efficacy of stenorel (Halofuginone). I. Against recent field isolates of six species of chicken Coccidia. *Poult. Sci.* **58**, 1469–1475 (1979).
- Lin, R. et al. Inhibition of Tgf-B signaling with halofuginone can enhance the antitumor effect of irradiation in Lewis lung cancer. *Oncotargets Ther.* **8**, 3549–3559 (2015).
- Juarez, P. et al. Halofuginone inhibits the establishment and progression of melanoma bone metastases. *Cancer Res.* **72**, 6247–6256 (2012).
- Marty, P. et al. Halofuginone regulates keloid fibroblast fibrotic response to Tgf-B induction. *Biomed. Pharmacother.* **135**, 111182 (2021).
- Cui, Z. et al. Halofuginone attenuates osteoarthritis by inhibition of Tgf-B activity and H-type vessel formation in subchondral bone. *Ann. Rheum. Dis.* **75**, 1714–1721 (2016).
- Assis, P. A. et al. Halofuginone inhibits phosphorylation of Smad-2 reducing angiogenesis and leukemia burden in an acute promyelocytic leukemia mouse model. *J. Exp. Clin. Cancer Res.* **34**, 65 (2015).
- Jain, P. P. et al. Halofuginone, a promising drug for treatment of pulmonary hypertension. *Br. J. Pharmacol.* **178**, 3373–3394 (2021).
- He, Y. Y. et al. Identification of hypoxia induced metabolism associated genes in pulmonary hypertension. *Front. Pharmacol.* **12**, 753727 (2021).
- Guignabert, C. & Humbert, M. Targeting transforming growth factor-B receptors in pulmonary hypertension. *Eur. Resp. J.* **57**, 2002341 (2021).
- Yue, Y. et al. Osthole inhibits cell proliferation by regulating the Tgf-B1/Smad/P38 signaling pathways in pulmonary arterial smooth muscle cells. *Biomed. Pharmacother.* **121**, 109640 (2020).

15. Bei, Y. et al. Long-term treatment with fasudil improves bleomycin-induced pulmonary fibrosis and pulmonary hypertension via inhibition of Smad2/3 phosphorylation. *Pulm. Pharmacol. Ther.* **26**, 635–643 (2013).
16. Yang, Z. et al. Tsantan sumtang restored right ventricular function in chronic hypoxia-induced pulmonary hypertension rats. *Front. Pharmacol.* **11**, 607384 (2021).
17. Bao, Y. R. et al. Sodium tanshinone II sulfonate ameliorates hypoxia-induced pulmonary hypertension. *Front. Pharmacol.* **11**, 687 (2020).
18. Florentin, J. et al. Inflammatory macrophage expansion in pulmonary hypertension depends upon mobilization of blood-borne monocytes. *J. Immunol.* **200**, 3612–3625 (2018).
19. Zhong, M., Zhang, X., Shi, X. & Zheng, C. Halofuginone inhibits Lps-induced attachment of monocytes to huvecs. *Int. Immunopharmacol.* **87**, 106753 (2020).
20. Liang, J. et al. Preventive effect of halofuginone on concanavalin a-induced liver fibrosis. *PLoS ONE*. **8**, e82232 (2013).
21. Sun, X. H., Fu, J. & Sun, D. Q. Halofuginone alleviates acute viral myocarditis in suckling Balb/C mice by inhibiting Tgf-B1. *Biochem. Biophys. Res. Commun.* **473**, 558–564 (2016).
22. Leiba, M. et al. Halofuginone inhibits Nf-Kappab and P38 Mapk in activated T cells. *J. Leukoc. Biol.* **80**, 399–406 (2006).
23. Huang, H., Kong, L., Luan, S., Qi, C. & Wu, F. Ligustrazine suppresses platelet-derived growth factor-BB-induced pulmonary artery smooth muscle cell proliferation and inflammation by regulating the PI3K/Akt signaling pathway. *Am. J. Chin. Med.* **49**, 437–459 (2021).
24. Quarck, R. et al. Characterization of proximal pulmonary arterial cells from chronic thromboembolic pulmonary hypertension patients. *Respir. Res.* **13**, 27 (2012).
25. Strzalka, W. & Ziemienowicz, A. Proliferating cell nuclear antigen (Pcna): A key factor in dna replication and cell cycle regulation. *Ann. Bot.* **107**, 1127–1140 (2011).
26. Gupta, V. K. & Chaudhuri, O. Mechanical regulation of cell-cycle progression and division. *Trends Cell Biol.* **32**, 773–785 (2022).
27. Lukasik, P., Zaluski, M. & Gutowska, I. Cyclin-dependent kinases (Cdk) and their role in diseases development-review. *Int. J. Mol. Sci.* **22**, 2935 (2021).
28. Pines, M. et al. Reduction in dermal fibrosis in the tight-skin (Tsk) mouse after local application of halofuginone. *Biochem. Pharmacol.* **62**, 1221–1227 (2001).
29. Xia, X. et al. Mir-31 shuttled by halofuginone-induced exosomes suppresses Mfc-7 cell proliferation by modulating the Hdac2/cell cycle signaling axis. *J. Cell. Physiol.* **234**, 18970–18984 (2019).
30. Lv, T. et al. Halofuginone enhances the anti-tumor effect of Ala-Pdt by suppressing Nrf2 signaling in Csc. *Photodiagn. Photodyn. Ther.* **37**, 102572 (2022).
31. Gnainsky, Y. et al. Involvement of the tyrosine phosphatase early gene of liver regeneration (Pr1-1) in cell cycle and in liver regeneration and fibrosis effect of halofuginone. *Cell Tissue Res.* **324**, 385–394 (2006).
32. Zhang, N., Dong, M., Luo, Y., Zhao, F. & Li, Y. Danshensu prevents hypoxic pulmonary hypertension in rats by inhibiting the proliferation of pulmonary artery smooth muscle cells via Tgf-B-Smad3-associated pathway. *Eur. J. Pharmacol.* **820**, 1–7 (2018).
33. Rol, N., Kurakula, K. B., Happe, C., Bogaard, H. J. & Goumans, M. J. Tgf-B and Bmpr2 signaling in Pah: Two black sheep in one family. *Int. J. Mol. Sci.* **19**, 2585 (2018).
34. Derynck, R. & Budi, E. H. Specificity, versatility, and control of Tgf-B family signaling. *Sci. Signal.* **12**, eaav5183 (2019).
35. Aashaq, S. et al. Tgf-B signaling: A recap of smad-independent and smad-dependent pathways. *J. Cell. Physiol.* **237**, 59–85 (2022).
36. Andre, P. et al. Therapeutic approaches for treating pulmonary arterial hypertension by correcting imbalanced Tgf-B superfamily signaling. *Front. Med.* **8**, 814222 (2022).
37. Li, L. et al. Tgf-B1 inhibits the apoptosis of pulmonary arterial smooth muscle cells and contributes to pulmonary vascular medial thickening via the Pi3K/Akt pathway. *Mol. Med. Rep.* **13**, 2751–2756 (2016).
38. Abeyrathna, P., Kovacs, L., Han, W. & Su, Y. Calpain-2 Activates Akt Via Tgf-B1-Mtorc2 Pathway in Pulmonary Artery Smooth Muscle Cells. *Am. J. Physiol.-Cell Physiol.* **311**, C24–C34 (2016).
39. Zhang, Y., Yuan, R. X. & Bao, D. Tgf-B1 promotes pulmonary arterial hypertension in rats via activating Rhoa/Rock signaling pathway. *Eur. Rev. Med. Pharmacol. Sci.* **24**, 4988–4996 (2020).
40. Li, Y. X., Run, L., Shi, T. & Zhang, Y. J. Ctrp9 regulates hypoxia-mediated human pulmonary artery smooth muscle cell proliferation, apoptosis and migration via Tgf-Beta1/Erk1/2 signaling pathway. *Biochem. Biophys. Res. Commun.* **490**, 1319–1325 (2017).
41. Wang, J. et al. The effect of halofuginone on cardiopulmonary function and its mechanism in rats with high-altitude pulmonary hypertension. *Tianjin. Med. J.* **51**, 41–44 (2023).
42. Jin, H. et al. Grape seed procyanidin extract attenuates hypoxic pulmonary hypertension by inhibiting oxidative stress and pulmonary arterial smooth muscle cells proliferation. *J. Nutr. Biochem.* **36**, 81–88 (2016).

### Author contributions

Rui Wang, Wu Li and Dongfeng Yin designed the research, provided funding and necessary facilities for experiments and revised the manuscript. Jiangtao Wang performed the experiments, analyzed the experimental data and drafted the manuscript. Lina Guan and Jian Yu analyzed the experimental data and drafted the manuscript. Bohua Ma, Huihua Shen, Guozhu Xing and Yawei Xu participated in the experiments. Qiufang Li and Juan Liu conducted the statistical analysis and revised the manuscript. Jia He and Yixuan Huang analyzed the data. Qin Xu and Wenhui Shi provided the animal modeling methods and experimental techniques. All authors approved the submission of this manuscript.

### Funding

This work was supported by the Xinjiang Uygur Autonomous Region Key R&D Task Special under Grant [Number 2022B03005].

### Declarations

### Competing interests

The authors declare no competing interests.

### Additional information

**Supplementary Information** The online version contains supplementary material available at <https://doi.org/10.1038/s41598-025-88258-z>.

**Correspondence** and requests for materials should be addressed to D.Y., W.L. or R.W.

**Reprints and permissions information** is available at [www.nature.com/reprints](http://www.nature.com/reprints).

**Publisher's note** Springer Nature remains neutral with regard to jurisdictional claims in published maps and institutional affiliations.

**Open Access** This article is licensed under a Creative Commons Attribution-NonCommercial-NoDerivatives 4.0 International License, which permits any non-commercial use, sharing, distribution and reproduction in any medium or format, as long as you give appropriate credit to the original author(s) and the source, provide a link to the Creative Commons licence, and indicate if you modified the licensed material. You do not have permission under this licence to share adapted material derived from this article or parts of it. The images or other third party material in this article are included in the article's Creative Commons licence, unless indicated otherwise in a credit line to the material. If material is not included in the article's Creative Commons licence and your intended use is not permitted by statutory regulation or exceeds the permitted use, you will need to obtain permission directly from the copyright holder. To view a copy of this licence, visit <http://creativecommons.org/licenses/by-nc-nd/4.0/>.

© The Author(s) 2025